



OPEN ACCESS

EDITED BY

Giovanna Battipaglia,
University of Campania Luigi Vanvitelli, Italy

REVIEWED BY

Hamada Ali,
Sultan Qaboos University, Oman
Wei-Bin Wang,
Shenyang Agricultural University, China

*CORRESPONDENCE

Lei Wang

✉ rockyking@163.com

Qing-Lai Dang

✉ qdang@lakeheadu.ca

RECEIVED 08 January 2024

ACCEPTED 26 March 2024

PUBLISHED 09 April 2024

CITATION

Wang L and Dang Q-L (2024) Elevated CO₂ and ammonium nitrogen promoted the plasticity of two maple in great lakes region by adjusting photosynthetic adaptation. *Front. Plant Sci.* 15:1367535. doi: 10.3389/fpls.2024.1367535

COPYRIGHT

© 2024 Wang and Dang. This is an open-access article distributed under the terms of the [Creative Commons Attribution License \(CC BY\)](https://creativecommons.org/licenses/by/4.0/). The use, distribution or reproduction in other forums is permitted, provided the original author(s) and the copyright owner(s) are credited and that the original publication in this journal is cited, in accordance with accepted academic practice. No use, distribution or reproduction is permitted which does not comply with these terms.

Elevated CO₂ and ammonium nitrogen promoted the plasticity of two maple in great lakes region by adjusting photosynthetic adaptation

Lei Wang^{1,2*} and Qing-Lai Dang^{2*}

¹Jiyang College, Zhejiang A&F University, Zhuji, Zhejiang, China, ²Faculty of Natural Resources Management, Lakehead University, Thunder Bay, ON, Canada

Introduction: Climate change-related CO₂ increases and different forms of nitrogen deposition are thought to affect the performance of plants, but their interactions have been poorly studied.

Methods: This study investigated the responses of photosynthesis and growth in two invasive maple species, amur maple (*Acer ginnala* Maxim.) and boxelder maple (*Acer negundo* L.), to elevated CO₂ (400 μmol mol⁻¹ (aCO₂) vs. 800 μmol mol⁻¹ (eCO₂) and different forms of nitrogen fertilization (100% nitrate, 100% ammonium, and an equal mix of the two) with pot experiment under controlled conditions.

Results and discussion: The results showed that eCO₂ significantly promoted photosynthesis, biomass, and stomatal conductance in both species. The biochemical limitation of photosynthesis was switched to RuBP regeneration (related to J_{max}) under eCO₂ from the Rubisco carboxylation limitation (related to V_{cmax}) under aCO₂. Both species maximized carbon gain by lower specific leaf area and higher N concentration than control treatment, indicating robust morphological plasticity. Ammonium was not conducive to growth under aCO₂, but it significantly promoted biomass and photosynthesis under eCO₂. When nitrate was the sole nitrogen source, eCO₂ significantly reduced N assimilation and growth. The total leaf N per tree was significantly higher in boxelder maple than in amur maple, while the carbon and nitrogen ratio was significantly lower in boxelder maple than in amur maple, suggesting that boxelder maple leaf litter may be more favorable for faster nutrient cycling. The results suggest that increases in ammonium under future elevated CO₂ will enhance the plasticity and adaptation of the two maple species.

KEYWORDS

global change, nitrogen form, amur maple, boxelder maple, photosynthetic adaptation

1 Introduction

Global change can affect the structure and productivity of ecosystems via its effects on the physiological processes of individual plants (Campoy et al., 2021). Elevated atmospheric CO₂, nitrogen (N) deposition and plant invasion are drivers of ecosystem changes (Bäurle et al., 2023; de Souza, 2023). A good understanding of plant phenotypic plasticity in response to elevated CO₂ and N deposition is essential for predicting the survival and growth of plant species under the predicted future climate conditions (Du et al., 2019; Liu et al., 2022).

Studies have shown that elevated CO₂ levels tend to have a fertilization effect on plants (Zhu et al., 2021). However, the increases in photosynthetic rate induced by elevated CO₂ do not necessarily always lead to increased biomass accumulation and growth (Skinner et al., 2018; Cabon et al., 2022; Green and Keenan, 2022). Elevated CO₂ can result in a downregulation of leaf photosynthetic capacity (maximum rate of ribulose-1,5-bisphosphate carboxylation, V_{cmax} ; maximum of photosynthetic electron transport rate, J_{max}) and stomatal conductance (g_s) (Sperry et al., 2019; Tcherkez et al., 2020). Photosynthetic downregulation under elevated CO₂ is generally resulted from increases in photosynthetic carbohydrate production and subsequent dilution in leaf nitrogen concentration (Yin et al., 2019). Under elevated CO₂, the limitation of photosynthesis in C3 plants can shift to RuBP regeneration (indicated by J_{max}) from Rubisco carboxylation (indicated by V_{cmax}) (Dusenge et al., 2019; Smith and Keenan, 2020) although co-limitation by the two processes is generally the norm in most C3 species (Smith and Keenan, 2020). Photosynthesis can also be limited by CO₂ diffusions, such as g_s and mesophyll conductance (g_m) (Sakoda et al., 2021). The adaptability of invasive tree species under elevated CO₂ should be fully explored.

Elevated CO₂ can inhibit the absorption and assimilation of nitrate but magnify the effects of ammonium addition (Domiciano et al., 2020). Elevated CO₂ may affect nitrate assimilation by inhibiting photorespiration because the assimilation process depends on reductants produced by photorespiration (Ainsworth and Long, 2021). Some studies suggest that elevated CO₂ directly inhibits the activity of nitrate reductase (Wujeska-Klaue et al., 2019). The relative abundance of ammonium and nitrate depends vary with soil type, microbial community, forest successional stage and atmospheric N deposition (Poucet et al., 2021; Wang et al., 2023). Ammonium is generally the main nitrogen source in late successional stages (Bloom, 2015). With the increasing proportion of ammonium in atmospheric N deposition, N source forms become more important in the study of plant response to climate change (Luo et al., 2022).

Plant invasion is also a driver of changes in plant communities associated with global change (Petruzzellis et al., 2021). Invasive plants can benefit more from elevated CO₂ than local species and hence climate change can further promote plant invasion and changes in species composition (Rathee et al., 2021). Plants usually have higher phenotypic plasticity in photosynthesis and biomass allocation, especially in key leaf traits (Specific leaf area (SLA), N_{area} , and net photosynthesis rate (A_n)) (Onoda et al., 2017;

Liu et al., 2022). Invasive plants also have higher capability for resource capture and utilization efficiency by reducing the cost of leaf construction (Barros et al., 2020). Plant invasion threatens biodiversity and ecosystem services (Petruzzellis et al., 2021). However, invasive plants can also lead to soil eutrophication and improve vegetation productivity (Lee et al., 2017). These paradoxes make it difficult to predict the response of plants to future global changes, especially elevated CO₂ and different forms of N deposition. It has been found that increases in ammonium in the soil are conducive to plant invasion, but its interaction with elevated CO₂ is poorly understood (Chen et al., 2021).

Amur maple (*Acer ginnala* Maxim.) is native tree species in northeast Asia and is popular as its leaves produce antioxidants similar to that of green tea (Bi et al., 2016). Amur maple has high ornamental value and is widely introduced in North America in the 1960s. Due to its tenacious adaptability, amur maple is listed as an invasive plant species by the Natural Resources Conservation Service and the Forestry Service of the United States Department of Agriculture (USDA, 2005). Boxelder maple (*A. negundo* L.) is a native pioneer tree species in North America with strong adaptability and has successfully invaded Europe, Asia, South America and Australia (Saccone et al., 2010; McEvoy et al., 2022). Boxelder maple has strong phenotypic plasticity and resource allocation ability but can promote the invasion by other species because of the fast nitrogen cycling of its litter (Porté et al., 2011). A recent genomic study suggests that boxelder maple has a smaller genome with recent gene family evolution which might be related to tendencies (McEvoy et al., 2022). However, there are few studies on the responses of these two invasive maple species to elevated CO₂ and N forms. The purpose of this study was to verify the following scientific questions: 1. Elevated CO₂ promoted the photosynthetic rate of two maple trees and changed the biochemical limits of photosynthesis; 2. The morphological plasticity of leaves was sensitive to climate change; 3. Compared with nitrate, ammonium nitrogen was conducive to the growth of two maple under elevated CO₂ condition.

2 Materials and methods

2.1 Plant materials and treatments

The seeds of Amur maple and boxelder maple were collected from 6 mature trees at least 50 m apart from each other in the natural forests (amur maple at 48.416N, 89.267W; boxelder maple at 48.429N, 89.261W) near Lakehead University Thunder Bay campus (Ontario, Canada). The seeds were stratified in wet sand at 4°C for about 60 days before being sown in germination trays. Seedlings with 10 cm high were transplanted into 4 L plastic pots filled with a mixture of vermiculite and peat moss (1:1, v:v) (Sun Gro[®], 770 Silver Street, Agawam, MA, USA) and were treated with different CO₂ and nitrogen form.

The experiment was conducted in four research greenhouses (G1, G2, G3, G4 see Table 1) on the Thunder Bay campus of Lakehead University. The experiment followed a split plot design with two [CO₂] levels [ambient 400 μmol mol⁻¹ (aCO₂) and elevated

800 $\mu\text{mol mol}^{-1}$ (eCO₂) as the main plot, and three nitrogen treatments as the split plot (10 mM ammonium, 10 mM nitrate, 10 mM N with equal proportion of ammonium and nitrate) (Table 1). The two tree species were nested within the N-CO₂ combination. Each CO₂ level had two replicates (two separate greenhouses). Each replicate of each treatment combination had 8 seedlings of each species (a total of 96 seedlings per species: 2 CO₂ * 2 replicates * 3 N forms * 8 seedlings).

The nitrogen sources used ammonium-sulfonate (NH₄)₂SO₄ for ammonium and sodium-nitrate NaNO₃ for nitrate (BioBasic Inc. 20 Konrad Crescent, Markham, ON, Canada). All N treatments received identical amounts of other nutrient elements: 5 mM Potassium phosphate and 4 g L⁻¹ Micromax Micronutrients Granular (Calcium 6%, Magnesium 3%, Sulphur 12%, Boron 0.1%, Copper 1%, Iron 17%, Manganese 2.5%, Molybdenum 0.05%, Zinc 1%) (Everris NA Inc. P.O. Box 3310, Dublin, OH, USA). The extra S provided with the ammonium formulation and the extra Na provided with the nitrate formulation were compensated in the nutrient solution to avoid differences in other elements between the different N treatments. The seedlings were fertilized twice a week and irrigated with 500 ml water within fertilizer according to the corresponding treatment every other day. The seedlings were randomly changed the position within the same greenhouse in each treatment every two weeks.

The CO₂ concentration in each greenhouse was maintained using by a CO₂ generator (GEN-2E, Custom Automated Products Inc., Riverside, California, USA). Other environmental conditions in all the greenhouses were 25/16°C (day/night) temperature, 50% RH and 16-h photoperiod. High-pressure sodium lamps (P.L. Systems, Grimsby, ON, Canada) were used to supplement then natural light when the ambient light intensity was below 500 $\mu\text{mol m}^{-2} \text{s}^{-1}$ or the natural daylength was shorter than 16-h. All the environmental variables in each greenhouse were monitored and

controlled by an Argus Titan Environment System (Argus Control Systems Ltd. Vancouver, BC, Canada).

2.2 Gas exchange and pigment measurement

After three months treatments, six seedlings were randomly selected from each treatment combination and foliar gas exchange was measured between 9:00 am and 16:00 pm on a unshaded mature leaf on the near the top of the canopy using a LI-6800 Portable Photosynthesis System (LI-COR Biosciences, 4647 Superior Street, Lincoln, Nebraska, USA). The gas exchange under treatment CO₂ was measured at the corresponding growth [CO₂] (aCO₂ at 400 $\mu\text{mol mol}^{-1}$, eCO₂ at 800 $\mu\text{mol mol}^{-1}$), 25°C temperature, 1.1 - 1.3 kPa water vapor pressure deficit, 1000 $\mu\text{mol m}^{-2} \text{s}^{-1}$ photosynthetically active radiation flux density. At least 30 minutes was allowed before a steady state reading was taken. The net photosynthetic rate (A_{n-g}), stomatal conductance (g_s), intercellular [CO₂] to ambient [CO₂] ratio (C_i/C_a), and photosynthetic nitrogen uses efficiency ($PNUE = A_{n-g}/N_{area}$) were subjected to statistical analyses.

Photosynthetic response to intercellular [CO₂] (A/C_i) curves were measured at 400, 300, 200, 100, 50, 400, 500, 600, 800, 1000, 1200, 1500 $\mu\text{mol mol}^{-1}$ [CO₂], 25°C temperature, 1.1 - 1.3 kPa VPD, and 1000 $\mu\text{mol m}^{-2} \text{s}^{-1}$ PAR. The maximum rate of Rubisco carboxylation V_{cmax} and maximum rate of photosynthetic electron transport J_{max} were estimated using the fitaci function, and the transition point (C_{i-t} , A_{n-t}) of biochemical limitation from Rubisco to RuBP regeneration was estimated using findCiTranstion function in the Plantecophys R package from A/C_i data (Duursma, 2015). The initial slope of A/C_i was estimated as apparent carboxylation efficiency (ACE), and the X-axis intercept was evaluated as the CO₂ compensation point (Γ_{ACi}).

TABLE 1 Outline of the experimental design and treatments.

Treatments	CO ₂ ($\mu\text{mol mol}^{-1}$)	Ammonium (mM)	Nitrate (mM)	Greenhouse	Amur maple (seedlings)	Boxelder maple (seedlings)
1	400	10		G1	8	8
1	400	10		G2	8	8
2	400	5	5	G1	8	8
2	400	5	5	G2	8	8
3	400		10	G1	8	8
3	400		10	G2	8	8
4	800	10		G3	8	8
4	800	10		G4	8	8
5	800	5	5	G3	8	8
5	800	5	5	G4	8	8
6	800		10	G3	8	8
6	800		10	G4	8	8

Nitrogen treatments are three levels of 10 mM ammonium, 5 mM ammonium & 5 mM nitrate, 10 mM nitrate. G1 and G2 are the two replicates greenhouse with ambient 400 $\mu\text{mol mol}^{-1}$ CO₂, G3 and G4 represent two replicates greenhouse with 800 $\mu\text{mol mol}^{-1}$ elevated CO₂.

The photosynthetic light response curve (lrc) was measured at 400 $\mu\text{mol mol}^{-1}$ [CO_2] and 1000, 1500, 1200, 900, 600, 300, 150, 50, 0 $\mu\text{mol m}^{-2} \text{s}^{-1}$ PAR (Figure 1A). Other measurement environment conditions were the same as A/C_i curve measurement. Curvature (θ) and photosynthetic rate of saturation light ($A_{n\text{-max}}$) were fitted from the lrc data by non-rectangular hyperbola model using non-linear least squares in R (Salter et al., 2019). The initial slope of the lrc was estimated as the apparent quantum yield (AQY) and the X-axis intercept was estimated as the light compensation point (LCP). The fitting line of A_n vs. C_i from lrc dataset (Figure 1B) was used to estimate $A_{n\text{-total}}$ by the Y-axis intercept and $A_{n\text{-total}}/C_a$ as the initial slope (Wang and Dang, 2023).

The initial line portions of three A/C_i were measured with 200, 150, 100, and 50 $\mu\text{mol mol}^{-1}$ of [CO_2], and 300, 150, and 75 $\mu\text{mol m}^{-2} \text{s}^{-1}$ PAR, from which the daytime respiratory rate (R_d) and intercellular CO_2 compensation point (C_i^*) were calculated using Walker's slope intercept method (Walker et al., 2016). The variable J method was employed to calculate mesophyll conductance (g_m) (Harley et al., 1992), using the equation $\Gamma^* = C_i^* + R_d/g_m$ (Walker et al., 2016), where Γ^* is the CO_2 compensation point in absence of day respiration.

After the gas exchange measurement, the tested leaves were immediately removed and stored in a refrigerator (-70°C). Leaf pigment was extracted using 80% acetone and the absorbance at 645 nm and 663 nm measured. Chlorophyll concentration (Chl) of the leaves was calculated with $Chl = 20.2 * A_{645} + 8.02 * A_{663}$ (Wellburn, 1994).

2.3 Relative photosynthetic limitation and nitrogen partitioning

The relative limitations of photosynthesis by biochemical (l_b), mesophyll conductance (l_m) and stomatal conductance (l_s) were calculated according to Grassi and Magnani (Grassi and Magnani, 2005): $l_b = g_t/(g_t + \partial A_n/\partial C_c)$; $l_s = (g_t/g_s * \partial A_n/\partial C_c)/(g_t + \partial A_n/\partial C_c)$; $l_m =$

$(g_t/g_m * \partial A_n/\partial C_c)/(g_t + \partial A_n/\partial C_c)$, where g_t is the total conductivity of CO_2 diffusion ($g_t = 1/(1/g_m + 1/g_s)$), $\partial A_n/\partial C_c$ is the initial slope of the A_n to C_c response curve and was calculated using the equation $\partial A_n/\partial C_c = V_{cmax}/(\Gamma^* + K_m)$ (Farquhar et al., 1980), where Γ^* was as noted previously and K_m was calculated by $K_m = K_c (1 + O/K_o)$ (Bernacchi et al., 2001).

We investigated the partitioning of leaf N into carboxylation (N_{cb}), electron transfer (N_{et}), light capture (N_{lc}) and respiration (N_{resp}). The calculation is based on Trouwborst's method (Trouwborst et al., 2011).

2.4 Biomass and nitrogen measurement

After three months CO_2 and nitrogen form treatments, the height of all the seedlings was measured. Leaf area was measured using a Regent WinFolia system (Regent Instruments Inc., Quebec City, QC, Canada). The seedlings were then harvested and separated into roots, stems, and leaves, and oven-dried at 75°C for 48 hours to constant weight to determine the biomass of different organs and specific leaf area (SLA). Leaf mass-based N concentration (N_{mass}) and carbon concentration (C) were measured using the dry combustion method on a CNS-2000 (LECO Corp., St. Joseph, MI, USA) at the Lakehead University Centre for Analytical Services. Area-based leaf N concentration (N_{area}) and total leaf N content per plant (N_{leaf}) were determined from leaf biomass and SLA.

2.5 Statistical analysis

The effects of CO_2 and N forms on photosynthetic and growth traits of individual tree species were investigated using two-way analysis of variance using the agricolae package in R. A three-way (CO_2 , N forms and species) ANOVA was performed for A_{n-g} and

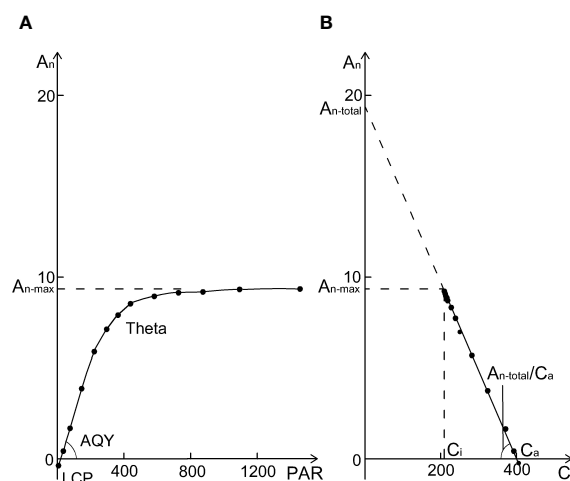


FIGURE 1

A sample of a photosynthetic light response curve (lrc) with relevant parameters (A) the photosynthetic rate at saturation light and 400 $\mu\text{mol mol}^{-1}$ CO_2 ($A_{n\text{-max}}$), the curvature of the lrc (Theta, θ), apparent quantum yield (the initial slope of lrc, AQY), and light compensation point (LCP). A_n vs. C_i derived from the lrc database (B), where $A_{n\text{-total}}$ and $A_{n\text{-total}}/C_a$ are the y-intercept and slope of the $A_n - C_i$ regression line. From (B), $A_{n\text{-total}}/C_a = A_{n\text{-max}}/(C_a - C_i)$, so $A_{n\text{-max}}/A_{n\text{-total}} = (C_a - C_i)/C_a$, which means that $A_{n\text{-max}}/A_{n\text{-total}} + C_i/C_a = 1$.

PNUE. Logarithmic or power transformation was used to transform variables that did not meet the normality and homogeneity assumptions before ANOVA was carried out. When an interaction was statistically significant, Tukey *post hoc* pairwise comparisons were conducted for the means. The principal component analysis (PCA) function of the FactoMineR package was used for PCA to investigate the relationship and clustering of physiological and growth-related parameters. The Bowen method (Bowen et al., 2017) was used to investigate the direct/indirect effects of CO₂ and N sources as categorical variables on biomass and A_{n-g} using the structural equation model (SEM) and the *psem* function in the piecewiseSEM package (Lefcheck, 2016). Based on the leaf economic spectroscopy (LES) and a prior structural model (Onoda et al., 2017; Liu et al., 2022), biomass was explained by A_{n-g} , N_{area} and *SLA*, and A_{n-g} was explained by photosynthetic capacity, *Chl* and g_t . The photosynthetic capacity was obtained by the regression equations from V_{cmax} and J_{max} . All the statistical analyses were performed using R.

3 Results

3.1 Growth in response CO₂ and N form

The eCO₂ significantly increased the biomass of both maple species but the effect was much bigger seedlings fertilized with NH₄ or a combination of NH₄ and NO₃ than those fertilized with NO₃ only (Figure 2). While the general response patterns were similar in the two species, there were differences in the responses between the two species: under the aCO₂, no significant effect of N form on the biomass was observed in amur maple (Figure 2A) but it was significantly lower in the boxelder maple seedlings that were supplied with ammonium only than those of seedlings that were fertilized with the other two N treatments (Figure 2B); Under eCO₂

treatment, the nitrate nitrogen only treatment significantly decreased the biomass of both maple species (Figure 2). CO₂ treatment significantly affected seedling height and leaf area (Tables 1, 3). However, these values of the boxelder maple were influenced by the interaction of the two treatments and showed a trend similar to that of biomass (Table 3). In general, the eCO₂ treatment significantly reduced *SLA*, except for amur maple treated with nitrate and boxelder maple treated with ammonium (Tables 2, 3).

3.2 Leaf nitrogen and PNUE

Treatment of eCO₂ significantly increased N_{area} in amur maple (Table 2) but not in boxelder maple (Table 3). In general, eCO₂ treatment promoted the N_{leaf} of the two tree species with the exception of boxelder maple fertilized with nitrate (Table 3). The eCO₂ treatment significantly promoted the leaf C/N value of boxelder maple (Table 3) but not of amur maple (Table 2).

Amur maple distributed relatively larger proportions of leaf N to N_{cb} , Net and N_c than did of boxelder maple while N allocation to N_{resp} was larger in boxelder maple than amur maple (Figure 3). Nitrate and eCO₂ treatment slightly limited leaf N allocation to carboxylation in both species (Figure 2). In general, the *PNUE* of boxelder maple was higher than that of amur maple, except for NN treatment under aCO₂ and nitrate treatment under eCO₂ (Figure 4A). Ammonium significantly reduced *PNUE* in amur maple under aCO₂ treatment (Figure 4A).

3.3 Photosynthesis traits

A_{n-g} was promoted by eCO₂ and its response in both tree species was similar to that of biomass under different treatments

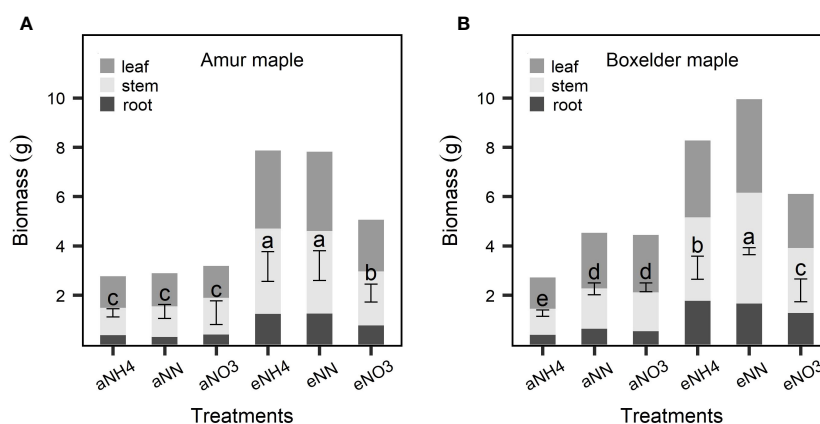


FIGURE 2

Biomass responses to CO₂ and N form treatments in amur maple (A) and boxelder maple (B). "a-" means ambient CO₂ (400 μmol mol⁻¹) and "e-" means elevated CO₂ (800 μmol mol⁻¹) treatments. NH₄: fertilized 10 mM (NH₄)₂SO₄; NN: fertilized with a combination of 5 mM (NH₄)₂SO₄ and 5 mM NaNO₃; NO₃: fertilized with 10 mM NaNO₃. Means (± SE, n=6) with different letters indicated significant differences between treatments (Tukey *post hoc* test, P<0.05).

TABLE 2 Height, leaf area, specific leaf area (SLA), and nitrogen-related traits of amur maple seedlings at ambient and elevated CO₂ in response to different forms of N supply.

CO ₂	N	Hight (cm)	Leaf area (cm ²)	SLA (cm ² g ⁻¹)	N _{area} (g m ⁻²)	N _{leaf} (mg plant ⁻¹)	C/N
aCO ₂	NH4	60.5 ± 3.1 c	286 ± 19 c	225 ± 6 a	1.1 ± 0.05 b	30.3 ± 3 c	19.9 ± 0.6 ab
	NN	74.5 ± 6 b	312 ± 35 c	233 ± 4 a	1.2 ± 0.03 ab	37.2 ± 4.2 bc	16.3 ± 0.4 c
	NO3	76.8 ± 4.8 b	301 ± 50 c	231 ± 5 a	1 ± 0.04 b	30.5 ± 4.8 c	19.2 ± 0.7 ab
eCO ₂	NH4	95.8 ± 2.2 a	654 ± 60 a	206 ± 4 b	1.3 ± 0.06 a	86.7 ± 11.7 a	17.5 ± 1 bc
	NN	95.5 ± 3.8 a	614 ± 55 a	192 ± 7 b	1.2 ± 0.08 ab	75 ± 9.1 a	20.2 ± 1.4 a
	NO3	93 ± 3.9 a	465 ± 32 b	223 ± 5 a	1.2 ± 0.04 ab	54.3 ± 5.3 b	17.7 ± 0.7 bc
P-value	CO ₂	< 0.001	< 0.001	< 0.001	0.005	< 0.001	0.994
	N	0.187	0.11	0.02	0.127	0.063	0.905
	CO ₂ : N	0.073	0.079	0.01	0.107	0.084	0.002

each value represents mean ± SE (n=6). Two-way ANOVA was performed to analyze CO₂ and nitrogen (N) as well as their interactive effects (CO₂: N). Significant effects (P ≤ 0.05) are marked in bold and “:” indicated interaction. Different letters within the same column indicated statistically significant differences between treatments (Tukey post hoc test, P<0.05). aCO₂: ambient CO₂ (400 μmol mol⁻¹); eCO₂: elevated CO₂ (800 μmol mol⁻¹); NH4: fertilized 10 mM (NH₄)₂SO₄; NN: fertilized 10 mM N with 5 mM (NH₄)₂SO₄ and 5 mM NaNO₃; NO3: fertilized 10 mM NaNO₃. SLA: specific leaf area; N_{area}: leaf N content based on leaf area; N_{leaf}: whole plant leaf N content; C/N: leaf carbon-nitrogen ratio.

(Figure 4B). The promoting effect of eCO₂ on A_{n-g} was smaller or not statistically significant under nitrate treatment (Figure 4B). Nitrate decreased both V_{max} and J_{max} in both species under eCO₂ although the effect was not always statistically significant but did not significantly affect either variable in either species aCO₂ treatment (Tables 4, 5). Ammonium significantly increased leaf Chl concentration of amur maple grown under eCO₂ (Table 4) while nitrate significantly increased leaf Chl of boxelder maple grown under aCO₂ (Table 5).

Nitrate significantly decreased g_m of amur maple under aCO₂ condition but increased it under eCO₂ (Table 4). In contrast, the g_m of boxelder maple was intermediate in seedlings fertilized with nitrate under eCO₂ while there was not significant difference among N treatments under aCO₂ (Table 5). C_i/C_a was generally higher in eCO₂ than under cCO₂, especially in boxelder maple (Tables 4, 5).

3.4 A/C_i traits and photosynthetic limitations

The transition point (C_{i-b} A_{n-t}) of photosynthetic limitation from Rubisco carboxylation to RuBP regeneration ion shifted to higher C_{i-g} and higher A_{n-g} under eCO₂ in both species (Figure 5). The transition point was much lower in amur maple seedlings fertilized with ammonium than other N treatments under aCO₂, but Γ_{ACi} was greater (Figures 5A–C). Ammonium significantly promoted (C_{i-g} A_{n-g}) and (C_{i-b} A_{n-t}) in amur maple (Figures 5D–F), nitrate lowered the transition point in boxelder maple under eCO₂ (Figures 5J–L).

Relative photosynthetic limitation analysis showed that photosynthesis was primarily limited by g_s in amur maple seedlings treated with aCO₂ and ammonium but primarily

TABLE 3 Hight, leaf area, specific leaf area (SLA), and nitrogen-related traits of boxelder maple grown at ambient and elevated CO₂ response different forms of N supply.

CO ₂	N	Hight (cm)	Leaf area (cm ²)	SLA (cm ² g ⁻¹)	N _{area} (g m ⁻²)	N _{leaf} (mg plant ⁻¹)	C/N
aCO ₂	NH4	45 ± 1.4 c	836 ± 74 d	600 ± 5.1 a	0.6 ± 0.05 b	52.1 ± 4.2 c	10.6 ± 0.2 b
	NN	52.8 ± 2.3 bc	1081 ± 91 cd	523 ± 11.5 bc	1 ± 0.09 a	106.1 ± 9.3 ab	8.9 ± 0.3 c
	NO3	56.2 ± 1.4 b	1293 ± 70 bc	557 ± 14.5 ab	0.8 ± 0.05 ab	104.1 ± 6.9 ab	9.2 ± 0.3 c
eCO ₂	NH4	70.7 ± 0.9 a	1435 ± 87 ab	518 ± 14 bc	0.9 ± 0.09 ab	123.6 ± 16.2 a	11.1 ± 0.6 ab
	NN	76 ± 1.8 a	1625 ± 54 a	438 ± 7.7 d	0.9 ± 0.04 ab	145.1 ± 4.3 a	11.1 ± 0.3 ab
	NO3	58.7 ± 2.8 b	1064 ± 127 cd	483 ± 8.6 cd	0.8 ± 0.17 ab	81 ± 11.2 bc	11.9 ± 0.7 a
P-value	CO ₂	< 0.001	< 0.001	< 0.001	0.565	< 0.001	< 0.001
	N	< 0.001	0.042	< 0.001	0.111	< 0.001	0.18
	CO ₂ : N	< 0.001	< 0.001	0.874	0.22	< 0.001	0.046

each value represents mean ± SE (n=6). Two-way ANOVA was performed to analyze CO₂ and nitrogen (N) as well as their interactive effects (CO₂: N). Significant effects (P ≤ 0.05) are shown in bold and “:” indicated interaction. Different letters within the same column indicated statistically significant differences between treatments (Tukey post hoc test, P<0.05). aCO₂: ambient CO₂ (400 μmol mol⁻¹); eCO₂: elevated CO₂ (800 μmol mol⁻¹); NH4: fertilized 10 mM (NH₄)₂SO₄; NN: fertilized 10 mM N with 5 mM (NH₄)₂SO₄ and 5 mM NaNO₃; NO3: fertilized 10 mM NaNO₃. SLA: specific leaf area; N_{area}: leaf N content based on leaf-area; N_{leaf}: whole plant leaf N content; C/N: leaf carbon-nitrogen ratio.

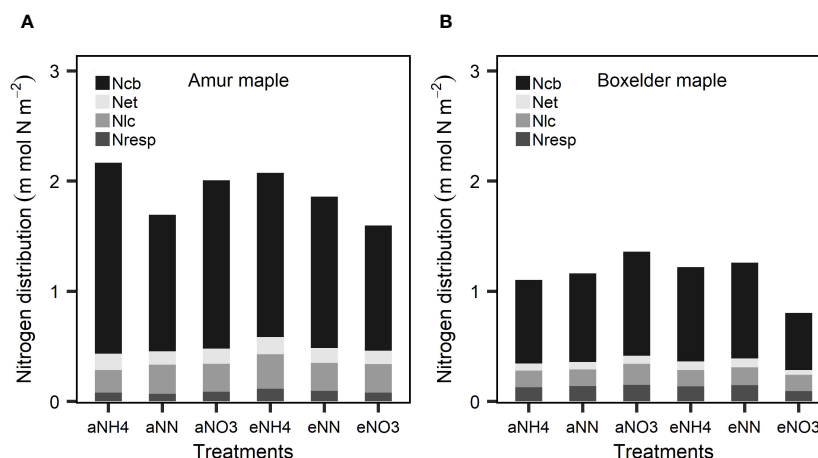


FIGURE 3

Leaf N partitioning into carboxylation (N_{cb}), electron transfer (N_{et}), light capture systems (N_{lc}), and respiratory (N_{resp}) in response to CO_2 and different N forms in amur maple (A) and boxelder maple (B). "a-" means ambient CO_2 ($400 \mu mol mol^{-1}$) and "e-" means elevated CO_2 ($800 \mu mol mol^{-1}$) treatments. NH4: fertilized with 10 mM $(NH_4)_2SO_4$; NN: fertilized with a combination of 5 mM $(NH_4)_2SO_4$ and 5 mM $NaNO_3$; NO3: fertilized with 10 mM $NaNO_3$.

limited by mesophyll conductance in all other treatment with the exception of seedlings treated with nitrate under eCO_2 where it was limited almost equally by mesophyll conductance and biochemistry (Figure 6A). In contrast, the photosynthesis of boxelder maple was mainly limited by biochemical and g_s (Figure 6B), particularly in the combination of nitrate and eCO_2 (Figure 6B).

3.5 Adaptation to CO_2 and N form

PCA showed an interesting result that the photosynthetic capacity parameters (V_{cmax} , J_{max}) did not orient to the ellipse of aCO_2 in the two species (Figures 7A, C). Seedlings grown under the eCO_2 were grouped into the ellipses with growth parameters (biomass and leaf area) and A_{n-g} (Figures 7A, C). It is also interesting to note that N_{area} and N_{leaf} clustered in the eCO_2 ellipse in amur maple (Figure 7A) while C/N clustered in the eCO_2 ellipse in boxelder maple (Figure 7B). Different N forms had no obvious effect on the response to CO_2 in amur maple since the three ellipses largely overlapped (Figure 7B). In boxelder maple, in contrast, nitrate clustered with N_{mass} and $A_{n-total}/C_a$, while the mixed N treatment was clustered with growth parameters (Figure 7D). It is worth noting that $A_{n-max}/A_{n-total}$ from lrc was negatively correlated with the growth parameters in both tree species at about 180-degree angles (Figures 7A–D), and a similar effect was found in SLA in boxelder maple (Figures 7C, D).

We constructed SEM (Structural Equation Model) to evaluate the direct/indirect effects on biomass and A_{n-g} by the two treatments (CO_2 and N) as categorical variables using piecewiseSEM package in R (Figures 8A, B). The results showed that CO_2 treatment had direct effects on the biomass of both tree species (Figures 8C, E), indirect effects on the biomass through N_{area} in amur maple (Figure 8C), and indirect effects on the biomass through A_{n-g} and SLA in boxelder maple (Figure 8E). N forms had a significant effect on the SLA in amur maple, but its impact on biomass did not reach

a significant level (Figure 8C). However, N treatment had a significant indirect effect on biomass through A_{n-g} and SLA in boxelder maple (Figure 8E).

CO_2 had a significant direct effect on the A_{n-g} of both maple (Figures 8D, F), and a significant indirect effect on the biomass through photosynthesis in amur maple (Figure 8D). No significant effect of N form was observed on A_{n-g} and related parameters in amur maple (Figure 8D, not shown). In boxelder maple, N treatment affected total CO_2 conductance, but had no significant effect on A_{n-g} (Figure 8F).

4 Discussion

4.1 Adaptation to elevated CO_2

Elevated CO_2 and associated climate change affect plant growth and distribution through via influencing physiological processes (Lauriks et al., 2022; Ma et al., 2023). Elevated CO_2 usually causes photosynthetic adaptation, which is typically manifested by decreases in photosynthetic capacity (V_{cmax} , J_{max}), N_{area} and g_s (Hao et al., 2023), but promotes biomass production and photosynthetic rate (Dusenge et al., 2020; Tcherkez et al., 2020). However, there was no reduction in photosynthetic capacity or N_{area} observed in either species in this study. To the contrary, eCO_2 increased V_{cmax} and J_{max} in seedlings fertilized with ammonium. The photosynthetic downregulation induced by eCO_2 is generally related to the dilution of leaf N and reduction in Rubisco as a result of increased carbohydrate production and growth (Dusenge et al., 2019).

Our PCA analysis shows that under aCO_2 treatment, both amur maple and boxelder maple converged on the ellipse in the direction of $A_{n-max}/A_{n-total}$ (the ratio of A_{n-max} and $A_{n-total}$ from lrc, see Figure 1B and Supplementary Table S1), and that $A_{n-max}/A_{n-total}$ was always inversely proportional to C_i/C_a . From Figure 1B, $A_{n-total}/$

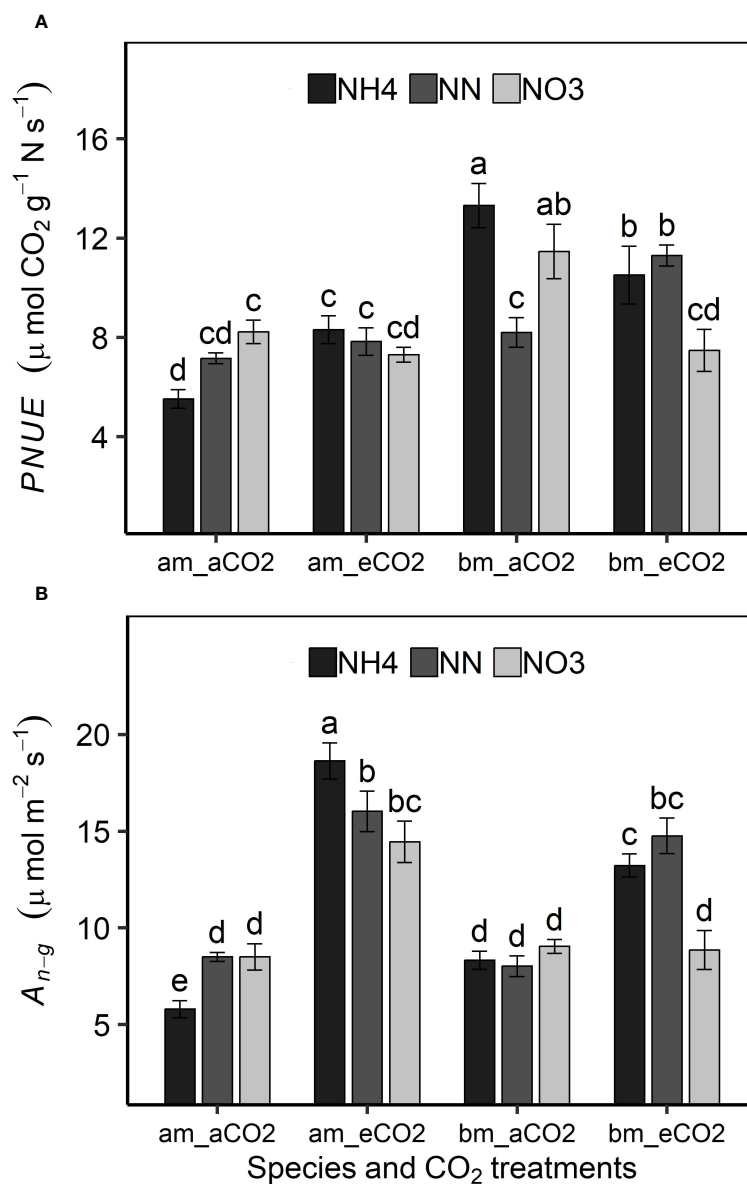


FIGURE 4

Effects of CO₂ and N forms on photosynthetic nitrogen use efficiency [PNUE, (A) and photosynthetic rate at growth CO₂ (A_{n-g} , (B))] in amur maple (am) and boxelder maple (bm). aCO₂: ambient CO₂ (400 $\mu\text{mol mol}^{-1}$); eCO₂: elevated CO₂ (800 $\mu\text{mol mol}^{-1}$); NH₄: fertilized with 10 mM (NH₄)₂SO₄; NN: fertilized with a combination of 5 mM (NH₄)₂SO₄ and 5 mM NaNO₃; NO₃: fertilized with 10 mM NaNO₃. Means (\pm SE, n=6) with different letters indicated significant differences between treatments (Tukey's test, P < 0.05).

$C_a = A_{n-max}/(C_a - C_i)$, so $A_{n-max}/A_{n-total} = (C_a - C_i)/C_a$, which means that $A_{n-max}/A_{n-total} + C_i/C_a = 1$. This seems to demonstrate an intrinsic inverse relationship between $A_{n-max}/A_{n-total}$ and C_i/C_a . Elevated CO₂ reduced $A_{n-max}/A_{n-total}$, but increased C_i/C_a in both species (Supplementary Tables S3, S4). These results indicated that the photosynthetic adaptation processes in two maple species appeared diverse and highly plastic (Moejles et al., 2017).

The SEM revealed that eCO₂ had positive effects on the biomass and A_{n-g} of both species, but only the effect on A_{n-g} in boxelder maple was statistically significant. CO₂ is considered as a signal to control stomatal movement and growth metabolisms (Hao et al., 2023). Our results show that the biomass of both maple species was closely related to A_{n-g} and CO₂ in the absence of other stresses.

4.2 Biochemical and CO₂ diffusion limitations to photosynthesis

This study shows that an important effect of eCO₂ is that it shifted the biochemical limitation of photosynthesis from Rubisco carboxylation to RuBP regeneration, i.e., from $A_{n-g} < A_{n-t}$ under aCO₂ to $A_{n-g} > A_{n-t}$ under eCO₂ (Wang et al., 2022). This result suggests that under the condition of the projected future climate, photosynthesis may be mainly limited by J_{max} rather than V_{cmax} (Smith and Keenan, 2020). It should be noted that when photosynthesis is limited by J_{max} , the sensitivity of A_n to C_i variation is reduced (Dusenge et al., 2019). The result that C_i/C_a ratio was higher under eCO₂ than under aCO₂ suggests that

TABLE 4 Photosynthetic capacity, chlorophyll concentration, conductance to CO₂ diffusion, and intercellular to external CO₂ concentration ratio in amur maple seedlings grown at ambient or elevated CO₂ in response to different forms of N source.

CO ₂	N	V_{cmax} ($\mu\text{ mol m}^{-2}\text{ s}^{-1}$)	J_{max} ($\mu\text{ mol m}^{-2}\text{ s}^{-1}$)	Chl (mg m^{-2})	g_m ($\text{mol m}^{-2}\text{ s}^{-1}$)	g_s ($\text{mmol m}^{-2}\text{ s}^{-1}$)	C_i/C_a
aCO ₂	NH ₄	73.1 ± 8.6 a	114 ± 6.1 b	412 ± 51 b	0.11 ± 0.01 a	77 ± 12.9 c	0.64 ± 0.03 ab
	NN	56.6 ± 1.2 bc	108 ± 3.3 b	507 ± 25 ab	0.07 ± 0.01 b	119 ± 4.2 bc	0.66 ± 0.01 ab
	NO ₃	69.2 ± 3.6 ab	119 ± 3.5 b	485 ± 36 b	0.05 ± 0 c	119 ± 9.6 bc	0.6 ± 0.02 b
eCO ₂	NH ₄	69.5 ± 1.9 a	140 ± 7.2 a	601 ± 24 a	0.04 ± 0 c	174 ± 12 a	0.73 ± 0.02 a
	NN	63.2 ± 3.1 ab	123 ± 8.5 ab	485 ± 37 b	0.04 ± 0.01 c	141 ± 23.7 ab	0.69 ± 0.04 ab
	NO ₃	48 ± 3.6 c	108 ± 8.4 b	497 ± 38 ab	0.08 ± 0.01 b	119 ± 20.8 bc	0.69 ± 0.03 ab
P-value	CO ₂	0.099	0.067	0.053	< 0.001	0.004	0.003
	N	0.013	0.1	0.912	0.133	0.758	0.301
	CO ₂ : N	0.0117	0.027	0.014	< 0.001	0.009	0.396

each value represents mean ± SE (n=6). Two-way ANOVA was performed to analyze CO₂ and nitrogen form (N) as well as their interactive effects (CO₂: N). Significant effects ($P \leq 0.05$) are marked in bold and “:” indicated interaction. Different letters within the same column indicated statistically significant differences between treatments (Tukey post hoc test, $P < 0.05$). aCO₂: ambient CO₂ (400 $\mu\text{mol mol}^{-1}$); eCO₂: elevated CO₂ (800 $\mu\text{mol mol}^{-1}$); NH₄: fertilized 10 mM (NH₄)₂SO₄; NN: fertilized 10 mM N with 5 mM (NH₄)₂SO₄ and 5 mM NaNO₃; NO₃: fertilized 10 mM NaNO₃. V_{cmax} : maximum rate of ribulose-1,5-bisphosphate carboxylation; J_{max} : maximum photosynthetic electron transport rate; Chl: leaf chlorophyll concentration. g_m : mesophyll conductance; g_s : stomatal conductance; C_i/C_a : intercellular (C_i) to ambient (C_a) CO₂ concentration ratio.

photosynthesis was less limited by CO₂ diffusion in the two species grown under eCO₂ (Lamba et al., 2018).

Photosynthetic capacity represents the CO₂ fixation potential of leaves and does not represent the photosynthetic rate under actual growth conditions (Wang et al., 2022), since the net photosynthetic rate of C3 plants is also affected by substrate CO₂ supply (Stefanski et al., 2020). For example, the photosynthetic capacity of amur maple treated with ammonium under aCO₂ was maintained at a high level, while the actual A_n was the lowest, which was obviously limited by low CO₂ supply and low stomatal conductance (Table 2, Figure 3A). Our results support the theory that higher photosynthetic capacity does not always translate into higher A_n (Xu et al., 2020).

The SEM showed that the resistance to CO₂ diffusion was not a primary driver for differences in A_n between treatments (Figures 8D, F) and the relationship appeared to be opposite between the two maple species. The resistance to CO₂ diffusion mainly includes g_s and g_m and has a significant effect on photosynthesis (Grassi and Magnani, 2005). However, using g_t [$g_t = g_s * g_m / (g_s + g_m)$] to express the overall conductivity of CO₂ seems to blur the individual effect of g_s or g_m (Grassi and Magnani, 2005). Although g_s and g_m jointly describe the diffusion of CO₂ from leaf surface to carboxylation sites, they are independent processes with different regulatory mechanisms and physiological significance. The g_s may be closely related to water status (Stefanski et al., 2020), while g_m integrates biochemical and

TABLE 5 Photosynthesis capacity, chlorophyll concentration, and CO₂ diffusion conductance in boxelder maple seedlings grown at ambient and elevated CO₂ in response to different forms of N source.

CO ₂	N	V_{cmax} ($\mu\text{ mol m}^{-2}\text{ s}^{-1}$)	J_{max} ($\mu\text{ mol m}^{-2}\text{ s}^{-1}$)	Chl (mg m^{-2})	g_m ($\text{mol m}^{-2}\text{ s}^{-1}$)	g_s ($\text{mmol m}^{-2}\text{ s}^{-1}$)	C_i/C_a
aCO ₂	NH ₄	34.9 ± 1.6 b	60.1 ± 1.9 ab	306 ± 21 b	0.09 ± 0.007 bc	60.2 ± 4.4 cd	0.64 ± 0.01 b
	NN	37.5 ± 1.8 b	59.7 ± 1.5 ab	297 ± 15 b	0.11 ± 0.004 bc	76.1 ± 7.1 ab	0.68 ± 0.02 b
	NO ₃	44 ± 1.1 a	67.2 ± 3.3 a	363 ± 21 a	0.09 ± 0.003 c	64.5 ± 4.5 cd	0.61 ± 0.02 b
eCO ₂	NH ₄	41.1 ± 0.8 ab	68.9 ± 3.4 a	306 ± 21 b	0.18 ± 0.017 a	84 ± 7.2 ab	0.78 ± 0.02 a
	NN	36 ± 3.4 b	66.4 ± 5.6 a	333 ± 14 ab	0.09 ± 0.004 c	89.7 ± 10.5 a	0.78 ± 0.02 a
	NO ₃	27.7 ± 3.1 c	47.8 ± 5.8 b	286 ± 14 b	0.12 ± 0.012 b	49.7 ± 6.6 d	0.7 ± 0.03 ab
P-value	CO ₂	0.038	0.692	0.365	< 0.001	0.199	< 0.001
	N	0.622	0.187	0.6	< 0.001	0.004	0.004
	CO ₂ : N	< 0.001	0.002	0.013	< 0.001	0.027	0.43

each value represents mean ± SE (n=6). Two-way ANOVA was performed to analyze CO₂ and nitrogen (N) as well as their interactive effects (CO₂: N). Significant effects ($P \leq 0.05$) are shown in bold and “:” indicated interaction. Different letters within the same column indicated statistically significant differences between treatments (Tukey post hoc test, $P < 0.05$). aCO₂: ambient CO₂ (400 $\mu\text{mol mol}^{-1}$); eCO₂: elevated CO₂ (800 $\mu\text{mol mol}^{-1}$); NH₄: fertilized 10 mM (NH₄)₂SO₄; NN: fertilized 10 mM N with 5 mM (NH₄)₂SO₄ and 5 mM NaNO₃; NO₃: fertilized 10 mM NaNO₃. V_{cmax} : maximum rate of ribulose-1,5-bisphosphate carboxylation; J_{max} : maximum photosynthetic electron transport rate; Chl: leaf chlorophyll concentration. g_m : mesophyll conductance; g_s : stomatal conductance; C_i/C_a : intercellular (C_i) to ambient (C_a) CO₂ concentration ratio.

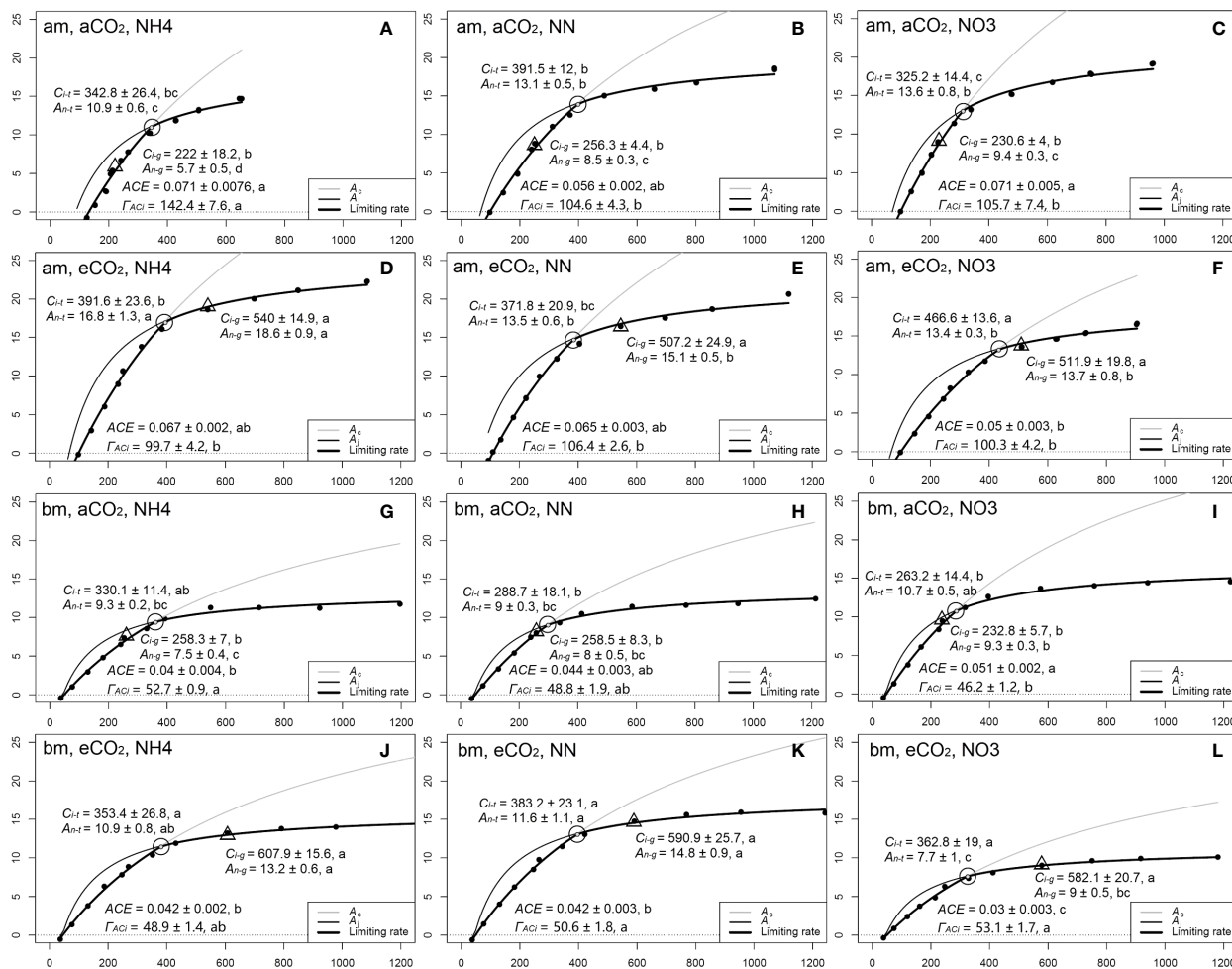


FIGURE 5

The A/C_i curves in response to different N forms in amur maple (am, A–F) and boxelder (bm, G–L) seedlings grown under ambient CO_2 (a CO_2 , A–C in am and G–I in bm) and elevated CO_2 (e CO_2 , D–F in am and J–L in bm). NH₄: fertilized with 10 mM (NH₄)₂SO₄ (left column); NN: fertilized with a combination of 5 mM (NH₄)₂SO₄ and 5 mM NaNO₃ (middle column); NO₃: fertilized with 10 mM NaNO₃ (right column). Each point denotes the means of six (C_{i-t} , A_{n-t}) values in A/C_i curve. The circles represent the transition point (C_{i-t} , A_{n-t}) from Rubisco carboxylation to RuBP regeneration of photosynthesis limitation. The triangles indicated the photosynthetic rate (C_{i-g} , A_{n-g}) under growth C_a (400 $\mu\text{mol mol}^{-1}$ versus 800 $\mu\text{mol mol}^{-1}$). ACE: apparent carboxylation efficiency estimated from the initial slope of A/C_i curve; Γ_{ACI} : CO_2 compensation point estimated from A/C_i curve intersects point on X-axis. Different letters of the same parameter in the same species are significantly different between treatments (Tukey post hoc test, $P < 0.05$, see Supplementary Table S2).

physical factors of intercellular CO_2 diffusion (Berghuijs et al., 2016).

4.3 N forms and partitioning effects

It is believed that e CO_2 is beneficial to plants that prefer ammonium over nitrate (Andrews et al., 2019; Dusenge et al., 2019). Our results show that ammonium fertilization led to the highest while nitrate resulted in the lowest photosynthesis and growth among the three fertilization treatments under e CO_2 . This result may be related to the lower energy consumption and higher metabolic efficiency of ammonium compared with nitrate (Bloom, 2015; Rubio-Asensio and Bloom, 2017). However, the accumulation of more ammonium in cells may cause ammonium toxicity, resulting in the decrease of g_s and A_n , chlorosis and growth

inhibition (Vega-Mas et al., 2017). Our results that Chl and g_s were lowest in seedlings fertilized with ammonium under a CO_2 may indicate a toxic effect of ammonium to those trees. Ammonium toxicity is attributed to excessive ammonium ions that lead to cell ion disturbances, the depletion of organic acid, and acid stress caused by the proton's mass formation (Hachiya et al., 2021). The e CO_2 can promote the synthesis of organic acids by providing the carbon framework and alleviating ammonium toxicity (Vega-Mas et al., 2017; La Peña et al., 2022). Our results showed that ammonium might be beneficial to the growth of the two maple species in the future when CO_2 is elevated. However, the mechanism of this synergistic effect of e CO_2 and ammonium needs further study.

It is common in C3 plants that e CO_2 inhibits the assimilation of nitrate (Rachmilevitch et al., 2004). The reason may be that e CO_2 inhibits photorespiration, and nitrate assimilation depends on

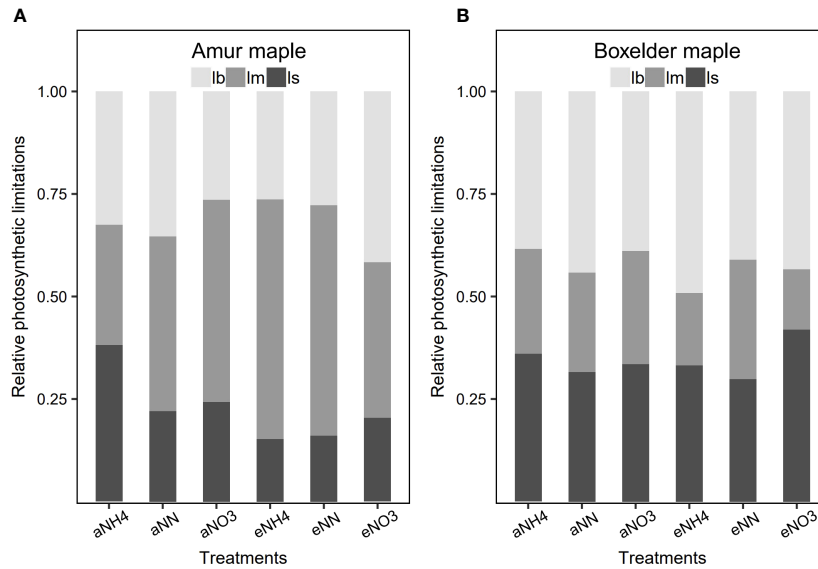


FIGURE 6
The relative photosynthesis limitations of biochemistry (l_b), stomatal resistance (l_s), and mesophyll resistance (l_m) in response to CO_2 and N form treatment in amur maple (A) and boxelder maple (B). Abbreviations are provided in [Supplementary Table S1](#).

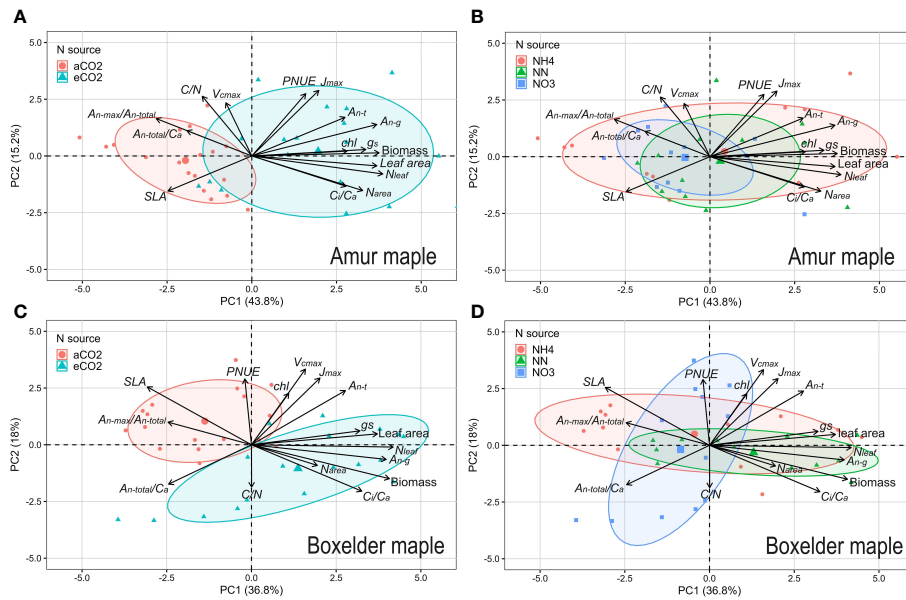


FIGURE 7
Principal Component Analysis (PCA) on growth and photosynthetic parameters in amur maple exposed to CO_2 (A) and N resource (B) treatments and in boxelder maple (C, D). The arrows point to near overlap, vertical, and reverse, which represent positive, no, and negative correlations between these parameters respectively. aCO₂: ambient CO_2 ($400 \mu mol mol^{-1}$); eCO₂: elevated CO_2 ($800 \mu mol mol^{-1}$); NH₄: fertilized 10 mM $(NH_4)_2SO_4$; NN: fertilized 10 mM N from 5 mM $(NH_4)_2SO_4$ and 5 mM $NaNO_3$; NO₃: fertilized 10 mM $NaNO_3$. J_{max} : maximum of photosynthetic electron transport rate; $PNUE$: photosynthesis nitrogen use efficiency; A_{n-t} : net photosynthesis rate at transition point (C_{i-t} , A_{n-t}) between Rubisco limitation and RuBP regeneration limitation based on A/C_i curve; A_{n-g} : net photosynthesis rate at a growth [CO_2] which eCO₂ at $800 \mu mol mol^{-1}$ and aCO₂ at $400 \mu mol mol^{-1}$; g_s : stomatal conductance; N_{leaf} : total N of the whole-plant leaf; chl : leaf chlorophyll concentration; C_i/C_a : the ratio of C_i and C_a ; N_{area} : leaf N per unit area; SLA : specific leaf area; $A_{n-max}/A_{n-total}$: the ratio of photosynthetic rate of saturation light at $400 \mu mol mol^{-1}$ (A_{n-max}) and the y-intercept of A_n vs. C_i fitting line ($A_{n-total}$) from light response curve database; $A_{n-total}/C_a$: the slope of A_n vs. C_i fitting line from light response curve database; C/N : leaf carbon and nitrogen ratio; V_{cmax} : maximum rate of ribulose-1,5-bisphosphate carboxylation; See [Supplementary Table S1](#) for other explanations.

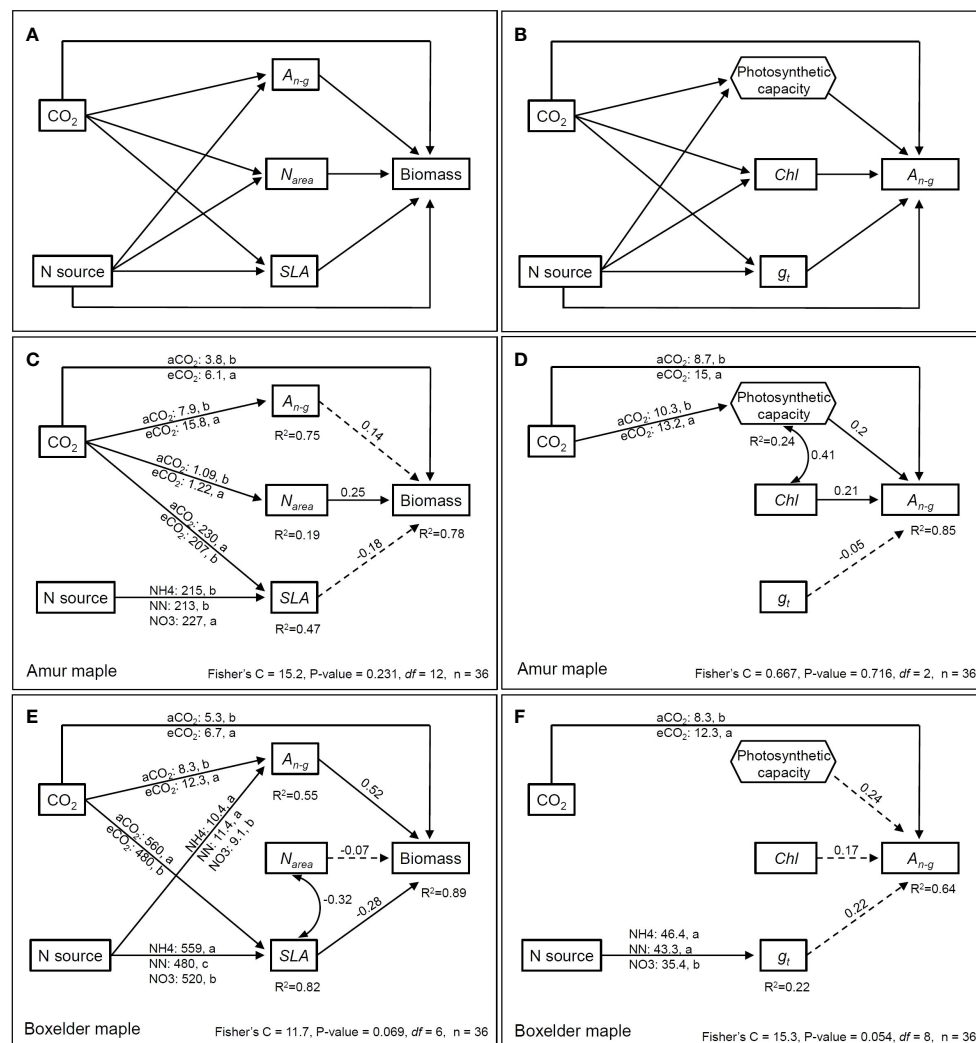


FIGURE 8

The *priori* (showing all tested paths) piecewise structural equation model (pSEM) relating to direct and indirect effects of CO₂ and N form on biomass (A) and A_{n-g} (B). Two CO₂ treatments (ambient CO₂: 400 μmol mol⁻¹ and elevated CO₂: 800 μmol mol⁻¹) and N source (10 mM N source by three forms: NH₄⁺, NH₄⁺+NO₃⁻ in 1:1, NO₃⁻) are treated as categorical variables. A_{n-g}: net photosynthesis rate at a growth [CO₂] which eCO₂ at 800 μmol mol⁻¹ and aCO₂ at 400 μmol mol⁻¹; N_{area}: leaf N per unit area; SLA: specific leaf area; Chl: leaf chlorophyll concentration; g_t: total conductance to CO₂ between the leaf surface and carboxylation sites (1/g_t = 1/g_s + 1/g_m). Multiple regression from V_{cmx} and J_{max} to A_{n-g} was used to construct photosynthetic capacity as a component variable (hexagonal frame). The SEM (using psem function in piecewiseSEM package R) of biomass and A_{n-g} in amur maple are in (C, D), while that of boxelder maple are in (E, F). Arrows mean the directional influence between the variables and the solid lines represent significant relationships, and the dashed lines refer to nonsignificant relationships (P > 0.05). The numbers on top of the arrows represent the standardized path coefficients (for continuous variables), and the numbers under the box with R² refer to the degree of variation of the variable interpreted by all paths. Curved double arrows represent a significant correlation between variables (with correlation coefficient). The values on the line from the categorical variable indicated the continuous variable estimated marginal means by the treatment levels.

photorespiration-related reductants (Ainsworth and Long, 2021). Furthermore, eCO₂ may also inhibit the activity of nitrate reductase (Wujeska-Klaue et al., 2019). The mixed nitrate and ammonium treatment appeared more beneficial to the growth of boxelder maple than the application of only nitrate, this suggests that ammonium and nitrate may have some interactive effects on boxelder maple. Notably, N allocation may also play an important role in the regulation of photosynthesis (Wang et al., 2021). Amur maple treated by aNH₄ and eNH₄ had equivalent N allocation to photosynthesis (Figure 4A), but the photosynthetic rate and biomass in the latter treatment were more than twice that of the former. This was probably because the N in the eNH₄ treatment

was distributed more evenly to different components such as N_{etb}, N_{lc} and N_{resp}, than in the aNH₄ treatment where there was a slight greater N allocation to N_{cb}.

4.4 Plasticity and leaf morphological traits

Invasive plants generally have higher plasticity because they exhibit favorable phenotypes and robust adaptability in response to changes in environmental conditions (Godoy et al., 2012; Liu et al., 2017). Plasticity is reflected in the trade-offs between leaf structure and physiological progress described in the leaf economic spectrum

(Liu et al., 2022), and in the optimal combination of key leaf traits SLA , N_{area} and A_n (Onoda et al., 2017). Successful invasive tree species often show higher SLA (lower leaf structure cost) and higher N_{area} (higher nutrient resources), which is often associated with higher efficiency of resource acquisition, higher photosynthetic rates and faster investment returns (Xiong and Flexas, 2018). Our results show that both amur maple and boxelder maple exposed to eCO_2 increased leaf construction cost (SLA lowered) and had higher N_{area} . The high phenotypic plasticity may further facilitate the spread of specific invasive species in the future when the atmospheric CO_2 elevation continues (Liu et al., 2017).

4.5 Adaptation strategy of amur maple and boxelder maple

Despite displaying comparable reactions to elevated CO_2 and different nitrogen sources in terms of biomass and leaf nitrogen allocation, Amur maple and boxelder maple seem to have adopted contrasting adaptation strategies for future climate change. Amur maple appears to prioritize maximizing photosynthetic capacity per unit area of leaves, whereas boxelder maple seems to excel in increasing biomass through adaptations in leaf morphology and nitrogen utilization efficiency (Supplementary Figures 3S, C). This trend is also evident in relative photosynthetic limitation (Figure 6) and structural equation models (Figures 8D, F).

Our results provide further support for the conclusions of previous studies that the great plasticity has facilitated the successful invasion of boxelder maple into Europe, Asia and South America (Porté et al., 2011; McEvoy et al., 2022). A study in Lithuania finds that boxelder maple facilitates invasion by increasing the rate of foliar decomposition and nutrient cycling (Manusadžianas et al., 2014). Our results showed that the C/N and N_{leaf} of boxelder maple were significantly higher than those of amur maple, suggesting that boxelder maple may speed soil nutrient cycling and the invasion of other species (Lee et al., 2017). A well-known paradox is that invasive plants reduce biodiversity but increase plant productivity (Rout and Callaway, 2009). A recent genomic comparison has found that boxelder maple has a smaller genome with recent gene family evolution which might be related to its robust adaptability (McEvoy et al., 2022). Even though the two maple trees have chosen different adaptation strategies for the future climate, they have both demonstrated a favorable reaction to the elevated CO_2 . It is important to note that the boxelder maple's strategy of optimizing leaf morphology and nitrogen utilization efficiency not only showcases its impressive phenotypic plasticity, but also enhances its invasive potential by facilitating nutrient cycling between leaves and soil.

5 Conclusions

Invasive tree species generally have greater plasticity and more efficient utilization of carbon and nitrogen sources in the environment. We found that amur maple and boxelder maple both showed strong plasticity in response to eCO_2 and variation

in N sources. Furthermore, they seem to exhibit a coordinated response to the two treatment factors. Ammonium was not conducive to the growth and physiology of both species under current CO_2 but significantly improved their performance under the elevated CO_2 . However, the effects of nitrate were the opposite. Boxelder maple seems to have stronger adaptability to future climate change than Amur maple. Because boxelder maple invests more N in its leaves and has a larger specific leaf area, indicating that boxelder maple could promote soil nutrient cycling and ecosystem function. We conclude that increases in soil ammonium will be beneficial to the plasticity and adaptation of amur maple and boxelder maple in the future as atmospheric CO_2 continues to rise.

Data availability statement

The raw data supporting the conclusions of this article will be made available by the authors, without undue reservation.

Author contributions

LW: Data curation, Formal analysis, Investigation, Writing – original draft, Writing – review & editing. Q-LD: Conceptualization, Funding acquisition, Investigation, Methodology, Project administration, Resources, Software, Supervision, Validation, Writing – review & editing.

Funding

The author(s) declare financial support was received for the research, authorship, and/or publication of this article. The study was supported by an NSERC Discovery Development Grant to Q-LD (Project No. DDG-2020-00008) and by Zhejiang A&U University Jiyang College Talent Initiation Project to LW (RC2023B06).

Acknowledgments

We want to thank Ms. Keri Pidgen, the Greenhouse Manager, for her logistic support and other operational assistance during the experiments.

Conflict of interest

The authors declare that the research was conducted in the absence of any commercial or financial relationships that could be construed as a potential conflict of interest.

The author(s) declared that they were an editorial board member of Frontiers, at the time of submission. This had no impact on the peer review process and the final decision.

Publisher's note

All claims expressed in this article are solely those of the authors and do not necessarily represent those of their affiliated organizations, or those of the publisher, the editors and the reviewers. Any product that may be evaluated in this article, or claim that may be made by its manufacturer, is not guaranteed or endorsed by the publisher.

Supplementary material

The Supplementary Material for this article can be found online at: <https://www.frontiersin.org/articles/10.3389/fpls.2024.1367535/full#supplementary-material>

SUPPLEMENTARY TABLE 1
Definition of acronyms.

SUPPLEMENTARY TABLE 2
ANOVA *P*-values of CO₂ and N source effects on photosynthetic parameters shown in Figure 4. Note: CO₂ treatment includes ambient CO₂ (400 μmol mol⁻¹) and elevated CO₂ (800 μmol mol⁻¹) and N treated with 10 mM N by three forms: NH₄⁺, NH₄⁺+NO₃⁻ in 1:1, NO₃⁻.

SUPPLEMENTARY TABLE 3
Photosynthetic parameters (mean ± SEM) derived from photosynthetic light response curves (LRC) in amur maple seedlings grown under different CO₂ and N forms. Note: each value represents mean ± SE (n=6). Two-way ANOVA was performed to analyze CO₂ and nitrogen (N) as well as their interactive effects (CO₂: N). Significant effects (*P* ≤ 0.05) are shown in bold and “:” indicated interaction. Different letters within the same column indicated statistically significant differences between treatments (Tukey *post hoc* test, *P* < 0.05). aCO₂: ambient CO₂ (400 μmol mol⁻¹); eCO₂: elevated CO₂ (800 μmol mol⁻¹); NH₄: fertilized 10 mM (NH₄)₂SO₄; NN: fertilized 10 mM N with 5 mM (NH₄)₂SO₄ and 5 mM NaNO₃; NO₃: fertilized 10 mM NaNO₃. Abbreviations are provided in Supplementary Table S1.

SUPPLEMENTARY TABLE 4
Photosynthetic parameters (mean ± SEM) derived from photosynthetic light response curves (LRC) in boxelder maple seedlings grown under different CO₂ and N forms. Note: each value represents mean ± SE (n=6). Two-way

ANOVA was performed to analyze CO₂ and nitrogen (N) as well as their interactive effects (CO₂: N). Significant effects (*P* ≤ 0.05) are shown in bold and “:” indicated interaction. Different letters within the same column indicated statistically significant differences between treatments (Tukey *post hoc* test, *P* < 0.05). aCO₂: ambient CO₂ (400 μmol mol⁻¹); eCO₂: elevated CO₂ (800 μmol mol⁻¹); NH₄: fertilized 10 mM (NH₄)₂SO₄; NN: fertilized 10 mM N with 5 mM (NH₄)₂SO₄ and 5 mM NaNO₃; NO₃: fertilized 10 mM NaNO₃. Abbreviations are provided in Supplementary Table S1.

SUPPLEMENTARY FIGURE 1
CO₂ concentration (A) and air temperature in (B) for the four climate-controlled glasshouses. The conditions were recorded 24 h a day every day. CO₂ setting was 800 μmol mol⁻¹ for the elevated and 400 μmol mol⁻¹ for the ambient treatment. Day 1 indicates the beginning of the experiment and Day 120 indicates the completion of the experiment.

SUPPLEMENTARY FIGURE 2
Pictures of amur maple (A) and boxelder maple (B) in different treatment combinations. “a-” means ambient CO₂ (400 μmol mol⁻¹) and “e-” means elevated CO₂ (800 μmol mol⁻¹) treatments. NH₄: fertilized 10 mM (NH₄)₂SO₄; NN: fertilized 10 mM N with 5 mM (NH₄)₂SO₄ and 5 mM NaNO₃; NO₃: fertilized 10 mM NaNO₃.

SUPPLEMENTARY FIGURE 3
Principal Component Analysis (PCA) on growth and photosynthetic parameters of seedlings exposed to CO₂ (A) and N resource (B) and in two species (C). The arrow direction of near overlap, vertical, and reverse, indicates positive correlation, no correlation, and negative correlation between these parameters, respectively. aCO₂: ambient CO₂ (400 μmol mol⁻¹); eCO₂: elevated CO₂ (800 μmol mol⁻¹); NH₄: fertilized 10 mM (NH₄)₂SO₄; NN: fertilized 10 mM N from 5 mM (NH₄)₂SO₄ and 5 mM NaNO₃; NO₃: fertilized 10 mM NaNO₃. *J*_{max}: maximum of photosynthetic electron transport rate; *P*_{NUE}: photosynthesis nitrogen use efficiency; *A*_{*n-t*}: net photosynthesis rate at transition point (*C*_{*i-t*}, *A*_{*n-t*}) between Rubisco limitation and RuBP regeneration limitation based on *A*/*C*_{*i*} curve; *A*_{*n-g*}: net photosynthesis rate at a growth [CO₂] which eCO₂ at 800 μmol mol⁻¹ and aCO₂ at 400 μmol mol⁻¹; *g*_{*s*}: stomatal conductance; *N*_{*leaf*}: total N of the whole-plant leaf; *Chl*: leaf chlorophyll concentration; *C*/*C*_{*a*}: the ratio of *C*_{*i*} and *C*_{*a*}; *N*_{*area*}: leaf N per unit area; *N*_{*mass*}: leaf N concentration; *SLA*: specific leaf area; *Γ*_{*ACi*}: CO₂ compensation point from *A*/*C*_{*i*} curve; *A*_{*n-max*}/*A*_{*n-total*}: the ratio of photosynthetic rate of saturation light at 400 μmol mol⁻¹ (*A*_{*n-max*}) and the y-intercept of *A*_{*n*} vs. *C*_{*i*} fitting line (*A*_{*n-total*}) from light response curve database; $\Delta A_n / \Delta C_{i-lrc}$: the slope of *A*_{*n*} vs. *C*_{*i*} fitting line from light response curve database; *C*/*N*: leaf carbon and nitrogen ratio; *V*_{*cmax*}: maximum rate of ribulose-1,5-bisphosphate carboxylation; *ACE*: apparent carboxylation efficiency. See Supplementary Table S1 for other explanations.

References

- Ainsworth, E. A., and Long, S. P. (2021). 30 years of free-air carbon dioxide enrichment (FACE): What have we learned about future crop productivity and its potential for adaptation? *Glob. Chang. Biol.* 27, 27–49. doi: 10.1111/gcb.15375
- Andrews, M., Condon, L. M., Kemp, P. D., Topping, J. F., Lindsey, K., Hodge, S., et al. (2019). Elevated CO₂ effects on nitrogen assimilation and growth of C3 vascular plants are similar regardless of N-form assimilated. *J. Exp. Bot.* 70, 683–690. doi: 10.1093/jxb/ery371
- Barros, V., Melo, A., Santos, M., Nogueira, L., Frosi, G., and Santos, M. G. (2020). Different resource-use strategies of invasive and native woody species from a seasonally dry tropical forest under drought stress and recovery. *Plant Physiol. Biochem.* 147, 181–190. doi: 10.1016/j.plaphy.2019.12.018
- Bäurle, I., Laplace, L., and Martin, A. (2023). Preparing for an uncertain future: molecular responses of plants facing climate change. *J. Exp. Bot.* 74, 1297–1302. doi: 10.1093/jxb/erac493
- Berghuijs, H. N. C., Yin, X., Ho, Q. T., Driever, S. M., Retta, M. A., Nicolai, B. M., et al. (2016). Mesophyll conductance and reaction-diffusion models for CO₂ transport in C3 leaves: needs, opportunities and challenges. *Plant Sci.* 252, 62–75. doi: 10.1016/j.plantsci.2016.05.016
- Bernacchi, C. J., Singas, E. L., Pimentel, C., Portis, A. R. Jr., and Long, S. P. (2001). Improved temperature response functions for models of Rubisco-limited photosynthesis. *Plant Cell Environ.* 24, 253–259. doi: 10.1111/j.1365-3040.2001.00668.x
- Bi, W., He, C., Ma, Y., Shen, J., Zhang, L. H., Peng, Y., et al. (2016). Investigation of free amino acid, total phenolics, antioxidant activity and purine alkaloids to assess the health properties of non-Camellia tea. *Acta Pharm. Sin.* 37, 170–181. doi: 10.1016/j.apsb.2015.11.003
- Bloom, A. J. (2015). The increasing importance of distinguishing among plant nitrogen sources. *Curr. Opin. Plant Biol.* 25, 10–16. doi: 10.1016/j.cpb.2015.03.002
- Bowen, J. L., Kearns, P. J., Byrnes, J. E. K., Wigginton, S., Allen, W. J., Greenwood, M., et al. (2017). Lineage overwhelms environmental conditions in determining rhizosphere bacterial community structure in a cosmopolitan invasive plant. *Nat. Commun.* 8, 433. doi: 10.1038/s41467-017-00626-0
- Cabon, A., Kannenberg, S. A., Arain, A., Babst, F., Baldocchi, D., Belmecheri, S., et al. (2022). Cross-biome synthesis of source versus sink limits to tree growth. *Science* 376, 758–761. doi: 10.1126/science.abm4875
- Campoy, J. G., Lema, M., Fenollosa, E., Munné-Bosch, S., and Retuerto, R. (2021). Functional responses to climate change may increase invasive potential of *Carpobrotus edulis*. *Am. J. Bot.* 108, 1902–1916. doi: 10.1002/ajb2.1745
- Chen, H., Huang, X., Shi, W., Kronzucker, H. J., Hou, L., Yang, H., et al. (2021). Coordination of nitrogen uptake and assimilation favors the growth and competitiveness of moso bamboo over native tree species in high-NH₄⁺ environments. *J. Plant Physiol.* 266, 153508. doi: 10.1016/j.jplph.2021.153508

- de Souza, A. P. (2023). Dynamic responses of carbon assimilation and stomatal conductance in the future climate. *J. Exp. Bot.* 74, 2790–2793. doi: 10.1093/jxb/erad049
- Domiciano, D., Nery, F. C., de Carvalho, P. A., Prudente, D. O., de Souza, L. B., Chalfun-Júnior, A., et al. (2020). Nitrogen sources and CO₂ concentration synergistically affect the growth and metabolism of tobacco plants. *Photosynth. Res.* 144, 327–339. doi: 10.1007/s11200-020-00743-w
- Du, Q., Liu, T., Jiao, X., Song, X., Zhang, J., and Li, J. (2019). Leaf anatomical adaptations have central roles in photosynthetic acclimation to humidity. *J. Exp. Bot.* 70, 4949–4962. doi: 10.1093/jxb/erz238
- Dusenge, M. E., Duarte, A. G., and Way, D. A. (2019). Plant carbon metabolism and climate change: elevated CO₂ and temperature impacts on photosynthesis, photorespiration and respiration. *New Phytol.* 221, 32–49. doi: 10.1111/nph.15283
- Dusenge, M. E., Madhavji, S., and Way, D. A. (2020). Contrasting acclimation responses to elevated CO₂ and warming between an evergreen and a deciduous boreal conifer. *Glob. Chang. Biol.* 26, 3639–3657. doi: 10.1111/gcb.15084
- Duurmsma, R. A. (2015). Plantecophys—An R package for analyzing and modelling leaf gas exchange data. *PLoS One* 10, e0143346. doi: 10.1371/journal.pone.0143346
- Farquhar, G. D., von Caemmerer, S., and Berry, J. A. (1980). A biochemical model of photosynthetic CO₂ assimilation in leaves of C₃ species. *Planta* 149, 78–90. doi: 10.1007/BF00386231
- Godoy, O., Valladares, F., and Castro-Díez, P. (2012). The relative importance for plant invasiveness of trait means, and their plasticity and integration in a multivariate framework. *New Phytol.* 195, 912–922. doi: 10.1111/j.1469-8137.2012.04205.x
- Grassi, G., and Magnani, F. (2005). Stomatal, mesophyll conductance and biochemical limitations to photosynthesis as affected by drought and leaf ontogeny in ash and oak trees. *Environ. Exp. Bot.* 28, 834–849. doi: 10.1111/j.1365-3040.2005.01333.x
- Green, J. K., and Keenan, T. F. (2022). The limits of forest carbon sequestration. *Science* 376, 692–693. doi: 10.1126/science.abo6547
- Hachiya, T., Inaba, J., Wakazaki, M., Sato, M., Toyooka, K., Miyagi, A., et al. (2021). Excessive ammonium assimilation by plastidic glutamine synthetase causes ammonium toxicity in *Arabidopsis thaliana*. *Nat. Commun.* 12, 4944. doi: 10.1038/s41467-021-25238-7
- Hao, L., Chang, Z., Lu, Y., Tian, Y., Zhou, H., Wang, Y., et al. (2023). Drought dampens the positive acclimation responses of leaf photosynthesis to elevated [CO₂] by altering stomatal traits, leaf anatomy, and Rubisco gene expression in *Pyrus*. *Environ. Exp. Bot.* 211, 105375. doi: 10.1016/j.envexpbot.2023.105375
- Harley, P. C., Loreto, F., Di Marco, G., and Sharkey, T. D. (1992). Theoretical considerations when estimating the mesophyll conductance to CO₂ flux by analysis of the response of photosynthesis to CO₂. *Plant Physiol.* 98, 1429–1436. doi: 10.1104/pp.98.4.1429
- Lamba, S., Hall, M., Råntfors, M., Chaudhary, N., Linder, S., Way, D., et al. (2018). Physiological acclimation dampens initial effects of elevated temperature and atmospheric CO₂ concentration in mature boreal Norway spruce. *Plant Cell Environ.* 41, 300–313. doi: 10.1111/pce.13079
- La Peña, M., Marín-Peña, A. J., Urmeneta, L., Coletto, I., Castillo-González, J., van Liempd, S. M., et al. (2022). Ammonium nutrition interacts with iron homeostasis in *Brachypodium distachyon*. *J. Exp. Bot.* 73, 263–274. doi: 10.1093/jxb/erab427
- Lauriks, F., Salomón, R. L., de Roo, L., Sobrino-Plata, J., Rodríguez-García, A., and Steppe, K. (2022). Limited mitigating effects of elevated CO₂ in young aspen trees to face drought stress. *Environ. Exp. Bot.* 201, 104942. doi: 10.1016/j.envexpbot.2022.104942
- Lee, M. R., Bernhardt, E. S., van Bodegom, P. M., Cornelissen, J. H. C., Kattge, J., Laughlin, D. C., et al. (2017). Invasive species' leaf traits and dissimilarity from natives shape their impact on nitrogen cycling: a meta-analysis. *New Phytol.* 213, 128–139. doi: 10.1111/nph.14115
- Lefcheck, J. S. (2016). piecewiseSEM: Piecewise structural equation modelling in R for ecology, evolution, and systematics. *Methods Ecol. Evol.* 7, 573–579. doi: 10.1111/2041-210X.12512
- Liu, Y., Oduor, A. M. O., Zhang, Z., Manea, A., Tooth, I. M., Leishman, M. R., et al. (2017). Do invasive alien plants benefit more from global environmental change than native plants? *Glob. Chang. Biol.* 23, 3363–3370. doi: 10.1111/gcb.13579
- Liu, H., Ye, Q., Simpson, K. J., Cui, E., and Xia, J. (2022). Can evolutionary history predict plant plastic responses to climate change? *New Phytol.* 235, 1260–1271. doi: 10.1111/nph.18194
- Luo, J.-J., Gao, Y.-M., Feng, W.-W., Liu, M.-C., Qu, B., Zhang, C., et al. (2022). Stronger ability to absorb nitrate and associated transporters in the invasive plant *Xanthium strumarium* compared with its native congener. *Environ. Exp. Bot.* 198, 104851. doi: 10.1016/j.envexpbot.2022.104851
- Ma, Y., Cao, B., Devi, M. J., Feng, X., Li, Y., Song, L., et al. (2023). Characterization of GALA (α -galactosidase) gene family and studying its response to elevated CO₂ in *Lycium barbarum*. *Environ. Exp. Bot.* 208, 105270. doi: 10.1016/j.envexpbot.2023.105270
- Manusadžianas, L., Darginavičienė, J., Gyltė, B., Jurkonienė, S., Krevš, A., Kuciškinė, A., et al. (2014). Ecotoxicity effects triggered in aquatic organisms by invasive *Acer negundo* and native *Alnus glutinosa* leaf leachates obtained in the process of aerobic decomposition. *Sci. Total. Environ.* 496, 35–44. doi: 10.1016/j.scitotenv.2014.07.005
- McEvoy, S. L., Sezen, U. U., Trouern-Trend, A., McMahon, S. M., Schaberg, P. G., Yang, J., et al. (2022). Strategies of tolerance reflected in two North American maple genomes. *Plant J.* 109, 1591–1613. doi: 10.1111/tpj.15657
- Moejes, F. W., Matuszyska, A., Adhikari, K., Bassi, R., Cariti, F., Cogne, G., et al. (2017). A systems-wide understanding of photosynthetic acclimation in algae and higher plants. *J. Exp. Bot.* 68, 2667–2681. doi: 10.1093/jxb/erx137
- Onoda, Y., Wright, I. J., Evans, J. R., Hikosaka, K., Kitajima, K., Niinemets, Ü., et al. (2017). Physiological and structural tradeoffs underlying the leaf economics spectrum. *New Phytol.* 214, 1447–1463. doi: 10.1111/nph.14496
- Petrzellis, F., Tordoni, E., Tomasella, M., Savi, T., Tonet, V., Palandrani, C., et al. (2021). Functional differentiation of invasive and native plants along a leaf efficiency/safety trade-off. *Environ. Exp. Bot.* 188, 104518. doi: 10.1016/j.envexpbot.2021.104518
- Porté, A. J., Lamarque, L. J., Lortie, C. J., Michalet, R., and Delzon, S. (2011). Invasive *Acer negundo* outperforms native species in non-limiting resource environments due to its higher phenotypic plasticity. *BMC Ecol.* 11, 28. doi: 10.1186/1472-6785-11-28
- Poucet, T., González-Moro, M. B., Cabasson, C., Beauvoit, B., Gibon, Y., Dieuaide-Noubhani, M., et al. (2021). Ammonium supply induces differential metabolic adaptive responses in tomato according to leaf phenological stage. *J. Exp. Bot.* 72, 3185–3199. doi: 10.1093/jxb/erab057
- Rachmilevitch, S., Cousins, A. B., and Bloom, A. J. (2004). Nitrate assimilation in plant shoots depends on photorespiration. *Proc. Natl. Acad. Sci. U.S.A.* 101, 11506–11510. doi: 10.1073/pnas.0404388101
- Rathee, S., Ahmad, M., Sharma, P., Singh, H. P., Batish, D. R., Kaur, S., et al. (2021). Biomass allocation and phenotypic plasticity are key elements of successful invasion of *Parthenium hysterophorus* at high elevation. *Environ. Exp. Bot.* 184, 104392. doi: 10.1016/j.envexpbot.2021.104392
- Rout, M. E., and Callaway, R. M. (2009). An invasive plant paradox. *Science* 324, 734–735. doi: 10.1029/2003GL019334
- Rubio-Asensio, J. S., and Bloom, A. J. (2017). Inorganic nitrogen form: a major player in wheat and *Arabidopsis* responses to elevated CO₂. *J. Exp. Bot.* 68, 2611–2625. doi: 10.1093/jxb/erw465
- Saccone, P., Pagès, J.-P., Girel, J., Brun, J.-J., and Michalet, R. (2010). *Acer negundo* invasion along a successional gradient: early direct facilitation by native pioneers and late indirect facilitation by conspecifics. *New Phytol.* 187, 831–842. doi: 10.1111/j.1469-8137.2010.03289.x
- Sakoda, K., Yamori, W., Groszmann, M., and Evans, J. R. (2021). Stomatal, mesophyll conductance, and biochemical limitations to photosynthesis during induction. *Plant Physiol.* 185, 146–160. doi: 10.1093/plphys/kiab011
- Salter, W. T., Merchant, A. M., Richards, R. A., Trethowan, R., and Buckley, T. N. (2019). Rate of photosynthetic induction in fluctuating light varies widely among genotypes of wheat. *J. Exp. Bot.* 70, 2787–2796. doi: 10.1093/jxb/erz100
- Skinner, C. B., Poulsen, C. J., and Mankin, J. S. (2018). Amplification of heat extremes by plant CO₂ physiological forcing. *Nat. Commun.* 9, 1094. doi: 10.1038/s41467-018-03472-w
- Smith, N. G., and Keenan, T. F. (2020). Mechanisms underlying leaf photosynthetic acclimation to warming and elevated CO₂ as inferred from least-cost optimality theory. *Glob. Chang. Biol.* 26, 5202–5216. doi: 10.1111/gcb.15212
- Sperry, J. S., Venturas, M. D., Todd, H. N., Trugman, A. T., Anderegg, W. R., Wang, Y., et al. (2019). The impact of rising CO₂ and acclimation on the response of US forests to global warming. *Proc. Natl. Acad. Sci.* 116, 25734–25744. doi: 10.1073/pnas.1913072116
- Stefanski, A., Bermudez, R., Sendall, K. M., Montgomery, R. A., and Reich, P. B. (2020). Surprising lack of sensitivity of biochemical limitation of photosynthesis of nine tree species to open-air experimental warming and reduced rainfall in a southern boreal forest. *Glob. Chang. Biol.* 26, 746–759. doi: 10.1111/gcb.14805
- Tcherkez, G., Ben Mariem, S., Larraya, L., García-Mina, J. M., Zamarreño, A. M., Paradela, A., et al. (2020). Elevated CO₂ has concurrent effects on leaf and grain metabolism but minimal effects on yield in wheat. *J. Exp. Bot.* 71, 5990–6003. doi: 10.1093/jxb/eraa330
- Trouwborst, G., Hogewoning, S. W., Harbinson, J., and van Ieperen, W. (2011). Photosynthetic acclimation in relation to nitrogen allocation in cucumber leaves in response to changes in irradiance. *Physiol. Plant* 142, 157–169. doi: 10.1111/j.1399-3054.2011.01456.x
- USDA. (2005). Available at: <https://www.invasive.org/weedcd/pdfs/wow/armur-maple.pdf>.
- Vega-Mas, L., Pérez-Delgado, C. M., Marino, D., Fuentes-Mendizábal, T., González-Murua, C., Márquez, A. J., et al. (2017). Elevated CO₂ induces root defensive mechanisms in tomato plants when dealing with ammonium toxicity. *Plant Cell Physiol.* 58, 2112–2125. doi: 10.1093/pcp/pcx146
- Walker, B. J., Skabelund, D. C., Busch, F. A., and Ort, D. R. (2016). An improved approach for measuring the impact of multiple CO₂ conductances on the apparent photorespiratory CO₂ compensation point through slope-intercept regression. *Plant Cell Environ.* 39, 1198–1203. doi: 10.1111/pce.12722

- Wang, L., and Dang, Q.-L. (2023). CO₂ demand-supply coordination in photosynthesis reflecting the plant-environment interaction: extension and parameterization of demand function and supply function. *AJPS* 14, 220–245. doi: 10.4236/ajps.2023.142017
- Wang, S., Guan, K., Wang, Z., Ainsworth, E. A., Zheng, T., Townsend, P. A., et al. (2021). Unique contributions of chlorophyll and nitrogen to predict crop photosynthetic capacity from leaf spectroscopy. *J. Exp. Bot.* 72, 341–354. doi: 10.1093/jxb/eraa432
- Wang, L., Zheng, J., Wang, G., and Dang, Q.-L. (2022). Combined effects of elevated CO₂ and warmer temperature on limitations to photosynthesis and carbon sequestration in yellow birch. *Tree Physiol* 43, 379–389. doi: 10.1093/treephys/tpac128
- Wang, W., Zhu, Q., Dai, S., Meng, L., He, M., Chen, S., et al. (2023). Effects of *Solidago canadensis* L. @ on mineralization-immobilization turnover enhance its nitrogen competitiveness and invasiveness. *Sci. Total. Environ.* 882, 163641. doi: 10.1016/j.scitotenv.2023.163641
- Wellburn, A. R. (1994). The Spectral Determination of Chlorophylls a and b, as well as Total Carotenoids, Using Various Solvents with Spectrophotometers of Different Resolution. *J. Plant Physiol.* 144, 307–313. doi: 10.1016/S0176-1617(11)81192-2
- Wujeska-Klaue, A., Crous, K. Y., Ghannoum, O., and Ellsworth, D. S. (2019). Lower photorespiration in elevated CO₂ reduces leaf N concentrations in mature Eucalyptus trees in the field. *Glob. Chang. Biol.* 25, 1282–1295. doi: 10.1111/gcb.14555
- Xiong, D., and Flexas, J. (2018). Leaf economics spectrum in rice: leaf anatomical, biochemical, and physiological trait trade-offs. *J. Exp. Bot.* 69, 5599–5609. doi: 10.1093/jxb/ery322
- Xu, Y., Shang, B., Feng, Z., and Tarvainen, L. (2020). Effect of elevated ozone, nitrogen availability and mesophyll conductance on the temperature responses of leaf photosynthetic parameters in poplar. *Tree Physiol.* 40, 484–497. doi: 10.1093/treephys/tpaa007
- Yin, X., Schapendonk, A. H. C. M., and Struik, P. C. (2019). Exploring the optimum nitrogen partitioning to predict the acclimation of C3 leaf photosynthesis to varying growth conditions. *J. Exp. Bot.* 70, 2435–2447. doi: 10.1093/jxb/ery277
- Zhu, Z., Zeng, H., Myneni, R. B., Chen, C., Zhao, Q., Zha, J., et al. (2021). Comment on “Recent global decline of CO₂ fertilization effects on vegetation photosynthesis”. *Science* 373, eabg5673. doi: 10.1126/science.abg5673